

## Phase relationships at 30 kbar for quartz eclogite composition in CaO-MgO-Al<sub>2</sub>O<sub>3</sub>-SiO<sub>2</sub>-H<sub>2</sub>O with implications for subduction zone magmas

TOSHIMORI SEKINE, PETER J. WYLLIE AND DON R. BAKER<sup>1</sup>

Department of Geophysical Sciences

University of Chicago

Chicago, Illinois 60637

### Abstract

Synthetic starting material, corresponding to oceanic tholeiite (analysis wt. %: SiO<sub>2</sub>, 52.5; Al<sub>2</sub>O<sub>3</sub>, 15.6; MgO, 14.6; CaO, 17.3), was run in sealed capsules at 30 kbar with 3.5% to 32.5% H<sub>2</sub>O for comparison with the phase diagram previously reported for a natural gabbro-H<sub>2</sub>O. The subsolidus assemblage is zoisite-coesite-eclogite, with the solidus at 810°C. Coesite/quartz disappears just above the solidus, zoisite between 900° and 950°C, eclogite + liquid persists through a wider temperature interval, and clinopyroxene + liquid exists below the liquidus. The liquidus is at 1110°C with excess H<sub>2</sub>O, and 1360°C with 7.5% H<sub>2</sub>O. Compositions of glass, clinopyroxene, garnet and zoisite were measured by electron microprobe for runs with 7.5% H<sub>2</sub>O. Glass analyses could not be obtained for runs below 1050°C. Glass analyses for runs at 1100°C and 1200°C included values that could not represent original liquid compositions, suggesting that the liquid composition changes during the quench, for reasons not fully understood. Equilibrium compositions of liquids were calculated from estimated modes and mass balance. The equilibrium liquid paths for both model and natural-rock compositions diverge from the average chemical variation of the calc-alkaline rock series, with divergence greatest for about 20-25% liquid where SiO<sub>2</sub> content corresponds to that of andesite. Partial melting of quartz eclogite in subducted oceanic crust at 100 km depth would produce liquids with Ca/(Mg+Fe) higher than andesites. Therefore, andesite is not a primary magma from subducted oceanic crust deeper than amphibole breakdown.

### Introduction

As indicated in several recent reviews, the magmatic processes associated with subduction zones are complex (Green, 1981a, 1981b; Kay, 1980; Wyllie, 1978, 1979, 1981). The proposal that intermediate and acid calc-alkaline lavas were produced as primary magmas by partial melting of subducted, hydrated oceanic crust now has few adherents (Marsh, 1979), and variations on the hybridization scheme proposed by Nicholls and Ringwood (1973) appear to be more consistent with geochemical data. Anderson *et al.* (1978) concluded that exothermic dehydration reactions cooled the subducted crust to such an extent that it did not melt at all, but they revised their model by including the effects of convection in the overlying mantle wedge, and concluded that un-

der some conditions melting can occur in the oceanic crust (Anderson *et al.*, 1980). Determination of the liquid-crystal paths associated with the origin of andesites therefore begins with the partial melting of subducted oceanic crust.

One approach to the problem is to use a natural rock with composition corresponding to a subducted oceanic basalt, to determine the phase relationships through a range of pressures in the presence of various fluids, and to compare the results with those obtained for andesite starting material. Experimental melting studies of basalts and andesites at mantle pressures where amphibole is stable have been presented by Green (1972), Green and Ringwood (1972), Lambert and Wyllie (1972, 1974), Allen *et al.* (1975), Allen and Boettcher (1978), and Stern *et al.* (1975). For the melting of quartz eclogite in the presence of H<sub>2</sub>O at somewhat higher pressures, Stern and Wyllie (1978) combined their new data with the results of Green and Ringwood (1968, 1972), Green

<sup>1</sup>Present address; Department of Geosciences, 204 Deike Building, The Pennsylvania State University, University Park, Pennsylvania 16802.

(1972), Stern and Wyllie (1973), and Stern (1974), and presented composition paths for liquid, garnet and clinopyroxene through the melting/crystallization interval of quartz eclogite with 5% H<sub>2</sub>O at 30 kbar.

Stern and Wyllie (1978) concluded that partial melting of quartz eclogite in subducted oceanic crust at 100 km depth produces liquids with a range of intermediate SiO<sub>2</sub> contents, but with Ca/(Mg+Fe) higher than the average composition trend of calc-alkaline dacite-andesite-basalt. The composition difference is not so great, however, that the conclusion is necessarily applicable to all basaltic compositions, including metasomatized basalts. Furthermore, there are severe experimental problems associated with determination of reversible equilibrium phase relationships for Fe-bearing rocks in the presence of volatile components (e.g., Merrill and Wyllie, 1973; Stern and Wyllie, 1975; Nehru and Wyllie, 1975; Green, 1976). Stern and Wyllie (1978) compensated for these problems as well as possible, but their results have an unknown margin of error imposed by the problems.

The study of whole rock compositions and of simple synthetic systems that include the major rock-forming minerals are complementary experimental approaches to petrogenetic problems. The system CaO–MgO–Al<sub>2</sub>O<sub>3</sub>–SiO<sub>2</sub> has been extensively studied as a model system for peridotites and basalts because it includes representatives of the major minerals occurring in these rocks. In this paper, we present the results obtained for a model quartz eclogite in the presence of H<sub>2</sub>O at 30 kbar, for comparison with the results obtained by Stern and Wyllie (1978) on a whole rock composition.

#### System CaO–MgO–Al<sub>2</sub>O<sub>3</sub>–SiO<sub>2</sub>–H<sub>2</sub>O

The geometrical framework for study of a model quartz eclogite is shown in Figure 1. The minerals encountered in the investigation are quartz/coesite, garnet with composition close to the join Py–Gr (pyrope–grossularite), clinopyroxene with composition close to the join Di–CaTs (diopside–lime Tschermak's molecule), kyanite, and zoisite. These mineral compositions are plotted in Figure 1. No amphibole was found. The triangle CaSiO<sub>3</sub>–MgSiO<sub>3</sub>–Al<sub>2</sub>O<sub>3</sub> includes the garnet join, and the compositional range of pyroxene solid solutions. The position of the triangle Gr<sub>2</sub>Py<sub>1</sub>–Gr<sub>1</sub>Py<sub>2</sub>–SiO<sub>2</sub> is also shown.

Stern and Wyllie (1978) considered the chemistry of andesites and other calc-alkaline rocks, and drew a compositional line on chemical variation diagrams which defined what is conventionally accepted as the

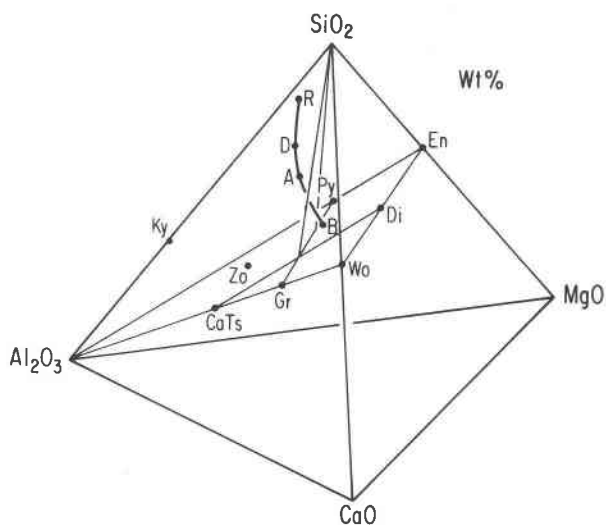


Fig. 1. System CaO–MgO–Al<sub>2</sub>O<sub>3</sub>–SiO<sub>2</sub> (weight percent) showing minerals involved in the experimental melting of a model quartz eclogite composition in the presence of H<sub>2</sub>O at 30 kbar. The curve BADR represents the average chemical variation of calc-alkaline rock series (see Stern and Wyllie, 1978). Only five components CaO, MgO+FeO, Al<sub>2</sub>O<sub>3</sub>, SiO<sub>2</sub> are recalculated to 100%, and FeO is added as equimolar MgO. The curve pierces the plane Gr<sub>2</sub>Py<sub>1</sub> (intersection of Di–CaTs and Py–Gr solid solutions)–Gr<sub>1</sub>Py<sub>2</sub> (intersection of two joins, Py–Gr and En–CaTs)–Qz between compositions B and A. The points B, A, D, and R are the projected positions of specific rocks: B = gabbro (Table 1, No. 4), A = tonalite (Stern and Wyllie, 1978), D = average composition of Nasu volcanic zone with range of SiO<sub>2</sub> from 65.0 to 67.5 (Yagi et al., 1963), and R = granite (Stern et al., 1975). The model quartz eclogite composition is close to point B (see Fig. 3). Abbreviations: Wo = wollastonite, Di = diopside, En = enstatite, Gr = grossularite, Py = pyrope, CaTs = lime Tschermak's molecule, Zo = zoisite, and Ky = kyanite.

average chemical variation of calc-alkaline rocks (e.g., Carmichael *et al.*, 1974, Figure 12-2). This chemical variation projects into Figure 1 as the curve B–A–D–R (basalt–andesite–dacite–rhyolite). Rock compositions are projected into the tetrahedron on the basis of the five components CaO–FeO–MgO–Al<sub>2</sub>O<sub>3</sub>–SiO<sub>2</sub>, with FeO added to equimolar MgO and recalculated to 100 percent. Some examples of calculations are listed in Table 1. The basalt plots close to the eclogite plane, with a little excess SiO<sub>2</sub>. The main chemical variation is an increase of SiO<sub>2</sub> along B–A–D–R. The line crosses the garnet–quartz triangle between basalt and andesite. The position of the line can be visualized more precisely from the two projections in Figures 3A and B.

Table 1 compares the composition of the model quartz eclogite used in this investigation with the natural basalt used by Stern and Wyllie, the average oceanic tholeiite according to Engel *et al.* (1965), and

Table 1. Chemical compositions of starting materials and tholeiites

	1	2	3	4	5	6	7	8	9
SiO <sub>2</sub>	52.45	49.10	52.28	45.91	50.25	49.94	52.77	49.84	54.42
TiO <sub>2</sub>		1.45		0.94		1.51		2.52	
Al <sub>2</sub> O <sub>3</sub>	15.64	14.50	15.53	17.19	18.81	16.69	17.64	14.09	15.39
Fe <sub>2</sub> O <sub>3</sub>				2.33		2.01		3.06	
FeO		10.40*		7.67		6.90		8.61	
MnO				0.22				0.16	
MgO	14.56	7.80	14.68	7.48	12.89	7.28	11.78	8.52	14.58
CaO	17.34	11.50	17.29	13.54	18.05	11.86	17.81	10.41	15.61
Na <sub>2</sub> O		2.57		1.63		2.76		2.15	
K <sub>2</sub> O		0.13		0.14		0.16		0.38	
Total	99.99	97.45		97.04		99.11		99.74	
Oxide Prop. (mole %)									
1/4 SiO <sub>2</sub>	24.6	27.3	24.6	26.4	24.6	29.9	26.5	28.6	26.1
MgO+FeO	40.6	45.2	40.7	40.3	37.6	39.8	35.2	45.7	41.7
CaO	34.8	27.4	34.7	33.3	37.8	30.0	38.3	25.6	32.1
Al <sub>2</sub> O <sub>3</sub>	18.6	20.7	18.5	24.0	22.3	25.1	22.1	21.1	19.1
MgO+FeO	43.8	49.3	44.0	41.6	38.7	32.4	37.3	50.6	45.7
CaO	37.5	29.9	37.5	34.4	39.0	42.5	40.6	28.3	35.2
"Eclogite" norm									
Di	33.7	23.5	33.8	23.9	29.8	22.1	31.3	18.9	27.6
Px	CaTs	11.1	10.7	11.1	20.4	0.0	21.6		7.4
	En		3.4					4.5	
	Jd		17.5	11.8		19.9		14.9	
Ga	Gr	15.4	15.7	15.5	16.1	13.7	11.1	16.5	17.6
	Py	27.6	28.1	27.7	28.8	24.5	19.9	29.6	31.5
Qz		12.2	11.9	12.3	11.9	11.7	16.1	15.5	16.0

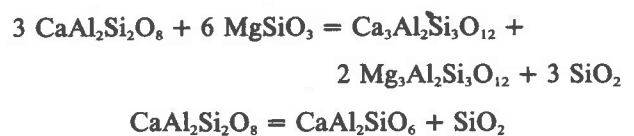
1. Simplified model quartz eclogite composition studied in this paper.
2. Basaltic rock from the Mid-Atlantic Ridge 30°N (Kay et al., 1970).
3. Calculated composition of No. 2 on the basis of MgO=FeO+MgO and CaO=CaO+Na<sub>2</sub>O.
4. Gabbro studied by Stern and Wyllie (1978).
5. Calculated composition of No. 4 on the basis of MgO=FeO+MgO and CaO=CaO+Na<sub>2</sub>O.
6. Average oceanic tholeiite given by Engel et al. (1965)
7. Calculated composition of No. 6 on the basis of MgO=FeO+MgO and CaO=CaO+Na<sub>2</sub>O.
8. Average of Hawaiian tholeiites (Macdonald and Katsura, 1964).
9. Calculated composition of No. 8 on the basis of MgO=FeO+MgO and CaO=CaO+Na<sub>2</sub>O.

\*Total iron as FeO.

the average Hawaiian tholeiite presented by Macdonald and Katsura (1964). The model quartz eclogite has a composition corresponding to an oceanic tholeiite (see analysis 3).

The "eclogite norms" listed in Table 1 were calculated using only the six components in the system Na<sub>2</sub>O-CaO-MgO-FeO-Al<sub>2</sub>O<sub>3</sub>-SiO<sub>2</sub>, with the further simplification that MgO and FeO were treated as isomorphous components. The components jadeite,

anorthite, diopside, and enstatite were calculated and then transformed into grossularite, pyrope and lime Tschermak's molecule according to the following reactions:



If there was insufficient anorthite component, then some enstatite remained in the norm.

The advantages of using the model composition instead of a natural quartz eclogite are that the phase relationships can be depicted with geometrical precision in a tetrahedron, and that the problems associated with Fe loss and the effect of oxygen fugacity are avoided. The main disadvantage is that important components are absent. It is probably safe to assume that  $K_2O$  in the quartz eclogite would be almost completely partitioned into the liquid at temperatures very close to the solidus. However, the role of  $Na_2O$  and its distribution between liquid and clinopyroxene must be evaluated in supplementary experiments or calculations.

### Experimental and analytical methods

The starting material was a dehydrated gel with composition listed in Table 1, prepared by a method similar to that of Luth and Ingamells (1965) from pure Mg metal,  $CaCO_3$ ,  $Al(NO_3)_3 \cdot 9H_2O$ , and Ludox. Nominally dry powdered samples were sealed with known amounts of  $H_2O$  in platinum capsules, and run at 30 kbar in piston-cylinder apparatus using a half-inch diameter tungsten carbide pressure chamber with hardened steel liner. Furnace assemblages including pyrex glass were similar to those described by Huang and Wyllie (1975). The problem of friction and its correction was reduced by using assemblies of pressed NaCl instead of pyrex glass, following A. L. Boettcher (personal communication, 1978). The piston-in method was employed with no friction correction for the NaCl cell below  $1225^\circ C$ , and with  $-3$  kbar friction correction for the pyrex glass cell above  $1225^\circ C$  (Huang and Wyllie, 1975). Pressure is believed to be accurate to within  $\pm 5\%$ . Pt/Pt10%Rh thermocouples were used without correction for the effect of pressure on emf. Temperatures are precise to  $\pm 5^\circ C$  and probably accurate to within  $\pm 13^\circ C$ . The added amount of water is believed to be accurate to within  $\pm 10\%$  relative.

The powdered gel sample is hygroscopic and contains 2.6 wt.%  $H_2O$ , measured by weight loss after firing to  $1000^\circ C$ . After ignition and during storage in a desiccator, the gel adsorbed 2%  $H_2O$  within 2 days. In view of the difficulty of preserving anhydrous gel, we used the gel directly from the desiccator, and incorporated the mass of adsorbed  $H_2O$ . Thus, adding 5%  $H_2O$  gave a charge containing  $7.6 \pm 0.5\%$   $H_2O$ .

It was determined in exploratory runs using previously crystallized gels that, in the presence of  $H_2O$ , the same run products were obtained from both crys-

talline and gel starting materials. Therefore, we conclude that for this composition at 30 kbar in the presence of  $H_2O$ , the gel does not exhibit its well-known characteristic to promote metastable crystallization. Run durations varied from a few hours to 2 days, with some runs of longer duration to test for reversibility, as listed in Table 2. The validity of some of the phase boundaries determined by synthesis runs using the gel starting mixture was confirmed by two-stage reversal runs. These runs are listed in Table 1 in pairs of rows, with the first row representing the first-stage synthesis run, and the second row showing the conditions to which the first run product was then subjected.

The run products were examined using standard optical and X-ray diffraction techniques. Analyses were obtained from the X-ray powder diffraction patterns for clinopyroxene (Herzberg, 1976) and garnet (Newton et al., 1977), using NaCl peaks (111), (200), and (220) as standards. Selected runs were analyzed by ARL electron microprobe for clinopyroxene, garnet, zoisite, kyanite, and glass. An energy-dispersive X-ray detector was used to accumulate the X-ray spectrum for 60 seconds. The integrated counts for Mg, Al, Si, and Ca, together with background readings, were read out and transferred to a mini-computer which made the instrumental and matrix corrections, and printed out weight percent and cation number on the basis of  $O = 24$ , using the program written by Ian Steele. Before measuring samples, MgO, CaO,  $Al_2O_3$ , and  $SiO_2$  contents were analyzed using standard glasses with compositions diopside, enstatite, and aluminous enstatite (5%, 10%, and 20%  $Al_2O_3$ ) to check reproducibility and precision. The analytical data obtained were repeated within  $\pm 1\%$  and were identical to the oxide contents of each glass within  $\pm 2\%$ . The accuracy of the microprobe analysis with energy-dispersive X-ray detector is considered to be  $\pm 2$  percent relative for elements greater than 5% concentration and  $\pm 5$  percent relative for elements less than 5% concentration (Reed and Ware, 1975).

### Experimental results

Experimental runs are listed in Table 2, and the results are plotted in Figure 2. The compositions of minerals estimated by X-ray methods are given in Table 2, and analyses of minerals and glass by electron microprobe are given in Tables 3 and 4. The compositions of phases through the melting/crystallization interval are plotted in two projections in Figures 3A and B.

Table 2. Experimental results of model quartz eclogite with water at 30 kbar

Run #	Temp. (°C)	wt% H <sub>2</sub> O	hrs.	Phases identified	X <sub>Gr</sub> (mole %) in Ga	
					X-Ray	Microprobe
BD001	1400	3.5	6	Cpx(t)+gl+q		
DB004	1300	3.5	20	Cpx+gl+q		
ST210	1250	3.5	4	Cpx+Ga(t)+gl+q		
ST144	1200	3.5	5	Cpx+Ga+gl	25	24
DB018	1100	3.5	20	Cpx+Ga+gl	25	
DB020	1000	3.5	24	Cpx+Ga(t)+gl+q		
ST203	900	3.5	43	Cpx+Ga+Qz+gl	21	
ST276	900	0.2*	71	Cpx+Ga+Qz+Zo(t)		
ST147	1350	7.5	1.7	Cpx(t)+gl+q		
ST145	1325	7.5	1.7	Cpx+gl+q		
ST014	1250	7.5	2	Cpx(t)+gl+q		
ST261	1200	7.5	6	Cpx+Ga(t)+gl		20
ST207	1100	7.5	4.5			
	1200		4	Cpx+gl+q		
ST143	1150	7.5	6	Cpx+Ga(t)+gl	26	
ST206	1200	7.5	3			
	1125		7	Cpx+Ga+gl+q		
ST254	1100	7.5	22	Cpx+Ga+gl		24
ST039	1050	7.5	17	Cpx+Ga+gl	30	26
ST256	1000	7.5	30	Cpx+Ga+gl		30
ST012	900	7.5	24	Cpx+Ga(t)+Zo(?) +gl	24	
ST258	1050	7.5	5			
	900		48	Cpx+Ga+Zo+gl		30
ST015	850	7.5	45	Cpx+Ga(t)+Qz(?) +Zo(?) +gl	19	
ST260	1000	7.5	20			
	800		78	Cpx+Ga+Qz+Zo(?) +Ky		26
DB006	1250	12.5	2	gl+q		
ST112	1200	12.5	22	Cpx+gl		
ST114	1150	12.5	6	Cpx+gl		
DB009	1100	12.0	16	Cpx+Ga+gl	25	
DB007	1000	12.5	26	Cpx+Ga+gl		
ST273	950	12.5	26	Cpx+Ga+gl		
ST274	850	12.5	18			
	950		31	Cpx+Ga+gl		
ST275	1000	12.5	18			
	900		25	Cpx+Ga+Zo(t)+gl		
ST202	1050	12.5	7			
	850		47	Cpx+Ga+Zo+gl	27	
ST154	775	12.5	117	Cpx+Qz+Ct+Zo(?) +V		
ST198	1050	12.5	7			
	775		64	Cpx+Ga+Qz+Ct(?) +Zo+V		
ST026	1150	22.5	6.5	gl+q		
ST142	1125	22.5	7	Cpx+gl		
ST030	1100	22.5	33	Cpx+gl+q		
ST141	1050	22.5	18.7	Cpx+Ga(t)+gl+V	25	
DB016	1000	22.5	10	Cpx+Ga+gl+V		
ST019	1125	28.0	8	gl		
ST122	1100	32.5	7.8	Cpx+gl+V+q		
ST118	1050	32.5	19.5	Cpx+Ga(t)+gl+V	28	
ST111	1000	32.5	19	Cpx+Ga(t)+gl+V		
ST146	825	32.5	64	Cpx+Ga+Qz(t)+Zo+Ct(?) +gl+V	25	

\*The starting material was a mixture of run products (Run #154, 198, and 260) dried at 110°C for 24 hours. Abbreviations, see Figure 2. gl = glass, q = quench crystals, (t) = trace, (?) suspected, not proved.

### Isobaric phase diagram for model quartz eclogite-H<sub>2</sub>O

Figure 2 shows the effect of H<sub>2</sub>O on the phase fields intersected at 30 kbar by the model quartz eclogite composition given in Table 1. The phase assemblages involve combinations of clinopyroxene, garnet, quartz, coesite, zoisite, liquid, and vapor. In the presence of excess vapor, the subsolidus assem-

blage of zoisite-coesite-eclogite begins to melt at a temperature between 800°C and 825°C, and melting is complete at 1110°C. Coesite/quartz melts a few degrees above the solidus, and the zoisite-out curve is between 900–950°C. The coesite-quartz boundary is from Stern and Wyllie (1978), because our runs were not definitive for this transition (see Table 2). Eclogite persists with liquid up to 1050–1100°C where

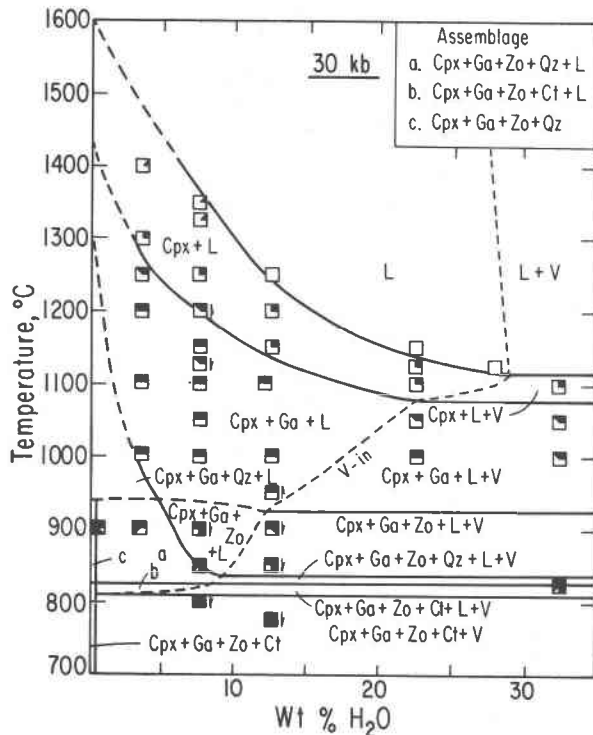


Fig. 2. Phase relationships at 30 kbar for the model quartz eclogite composition (Table 1) with varying  $H_2O$  contents (wt.%). The gel starting material contained 2.6 wt.%  $H_2O$ . The size of squares shows the range of accuracy of temperature and water weighed into capsules. Arrows indicate two-stage reversal runs. For experimental data see Table 2. The position of the vapor-in curve (dashed line) is uncertain. Abbreviations: L = liquid, V = vapor, and for others see Figure 1.

garnet disappears, leaving clinopyroxene with liquid through a narrow temperature interval to the liquidus.

The position of the vapor-out curve is drawn according to the presence or absence of vapor as listed in Table 2, and the criterion for vapor was detection of free water when the capsule was opened. However, vapor is exsolved from  $H_2O$ -undersaturated glasses during quench from high pressure (e.g., Boettcher and Wyllie, 1969), and we were unable to establish unambiguous criteria for the location of the vapor-out curve.

Within the vapor-absent region, the zoisite-out curve remains between the limits of the 900–950°C bracket. The other phase boundaries rise steeply with decreasing  $H_2O$  content to terminate within the undetermined melting interval for the anhydrous quartz eclogite composition. According to experimental data of Raheim and Green (1974, Table 3), the solidus for quartz eclogite is dependent upon  $Mg/(Mg+Fe^{2+})$ .

Using their data, the solidus of the anhydrous model quartz eclogite with  $Mg/(Mg+Fe^{2+}) = 1$  might be located above 1300°C at 30 kbar. Extrapolation of the liquidus boundary in Figure 2 indicates that the anhydrous liquidus for this composition may exceed 1500°C. With decreasing  $H_2O$  content, the temperature intervals for the fields of clinopyroxene + liquid and eclogite + liquid increase compared with the intervals for excess vapor. For low  $H_2O$  contents, the temperature interval above the solidus for the existence of quartz in the partially melted eclogite is greatly increased.

The vapor-absent subsolidus assemblage of zoisite-coesite/quartz-eclogite should exist for compositions with up to an estimated 0.2%  $H_2O$ . Melting of this assemblage does not begin at 800°C, but at a higher, undetermined temperature near 925°C, where zoisite breaks down releasing  $H_2O$  for a melting reaction.

Several two-stage runs were completed to test the positions of boundaries based on synthesis runs. With 7.5%  $H_2O$ , the position of the garnet-out phase boundary was confirmed by run 207, in which the first-stage assemblage of Cpx + Ga + L lost garnet after 4 hours at 1200°C. In run 206, garnet grew in the first-stage assemblage of Cpx + L after 7 hours at 1125°C (well below the plotted garnet-out boundary). A first-stage assemblage of Cpx + Ga + L produced zoisite in 48 hours at 900°C in run 258, with better crystal growth than in the 24-hour synthesis run (012). The same first-stage assemblage lowered to 800°C in run 260 contained quartz, kyanite, and suspected zoisite, with no detectable glass. Kyanite is probably metastable. Zoisite without kyanite was produced in runs 154 and 198 with 12.5%  $H_2O$  at 775°C.

#### Kyanite, quartz, coesite

Similar results were obtained for zoisite, quartz and coesite in two-stage runs with 12.5%  $H_2O$ . The first-stage assemblage of Cpx + Ga + L produced zoisite after 47 hours at 850°C (run 202), and after 64 hours at 775°C (run 198) zoisite was joined by quartz and possibly a trace of coesite, with no liquid remaining. The result for 117-hour synthesis run 154 at 775°C contained no garnet (with more coesite and less definite zoisite). We attribute the absence of garnet in the low-temperature synthesis run to sluggish nucleation, and we accept its occurrence in the two-stage run 198 as evidence that garnet is stable at 775°C. We know of no reaction in this bulk composition that would replace the stable garnet of 900°C

and above by other minerals at lower temperatures.

Zoisite did not grow in synthesis run 203 at 900°C with 3.5% H<sub>2</sub>O. We attribute this to slow reaction rates. Zoisite was present (detected by X-ray techniques in the products of run 276 at 900°C, with starting material a mixture of clinopyroxene, garnet, quartz, coesite, zoisite, and kyanite (run products of 154, 198, and 260 dried at 110°C for 24 hours). Neither kyanite nor coesite was identified. Therefore, we locate the zoisite-out boundary between 900–950°C with 3.5% H<sub>2</sub>O.

Zoisite is considered to be a subsolidus mineral rather than kyanite for the following reason. The grossularite component of the garnet in run 260, which contained kyanite, was poorer than that in run 258 (with zoisite), and the compositions of clinopyroxene in both runs are almost identical, except for a slight difference of Al<sub>2</sub>O<sub>3</sub> content. The modal proportions (weight percent) of the minerals in the subsolidus assemblage can be calculated if the solute in the vapor is neglected, or if it is assumed that the solute dissolves all components equally. The amount of each mineral is as follows: clinopyroxene, 42%; garnet, 33%; zoisite, 15%; coesite, 10%. If the subsolidus assemblage contained kyanite instead of zoisite (run 260), the proportions would change to: clinopyroxene, 66%; garnet, 14%; kyanite, 13%; coesite, 7%. Approximate modes of the subsolidus assemblages indicate that there are almost equal proportions of clinopyroxene and garnet, supporting the conclusion that zoisite is the stable mineral rather than kyanite.

#### Phase compositions

Tables 3 and 4 give microprobe analyses of phases in a series of runs with 7.5% H<sub>2</sub>O and in one run with 3.5% H<sub>2</sub>O. Compositions of garnets and clinopyroxenes were measured in most runs. Glass compositions

could not be measured in runs from 1050°C and below, containing relatively small amounts of interstitial liquid. The glasses analyzed contained no quench crystals. Overgrowth of clinopyroxene on the surfaces of primary crystals could cause changes in compositions of quenched glasses compared with original liquids (Green, 1973). The small size of clinopyroxene made measurements difficult in many runs. The compositions of garnets estimated from X-ray diffraction patterns are listed in Table 2 in terms of mole percent of grossular component. Analyses by electron microprobe are listed in Table 3. Results from X-ray and microprobe compared for run 144 and 039 in Table 2 show reasonable agreement. Zoisite composition was determined in run 258 (900°C).

Results from Tables 3 and 4 are projected from within the tetrahedron CaO–MgO–Al<sub>2</sub>O<sub>3</sub>–SiO<sub>2</sub> onto two planes in Figures 3A and B. The spatial relationships can be visualized by comparison of Figures 3 and 1. The curve shown in Figure 1 for the average chemical variation of calc-alkaline rocks is represented in Figure 3 by the narrow, shaded band B–A–D–R. The composition of the starting material, the model quartz eclogite, is given by point M.

As shown in Figures 3A and B, and in Table 3 for 3.5% H<sub>2</sub>O, the clinopyroxene in high-temperature, near-liquidus runs with H<sub>2</sub>O content of 7.5% and less is rich in Ca-Tschermak's molecule. With decreasing temperature, the clinopyroxene of the assemblage Cpx + L is enriched in the diopside component, with decrease in the percentage of the enstatite component. Within the temperature interval for the assemblage Cpx + Ga + L, the garnets are enriched in the grossular component, and the clinopyroxenes become Ca-rich. The mineral compositions are almost identical at 1000°C and 900°C, but at 800°C the components of grossular and Ca-Tschermak's mole-

Table 3. Chemical compositions, determined by microprobe analysis, of clinopyroxenes, garnets, and zoisite in the melting interval of model quartz eclogite at 30 kbar.

Run#	144	147	261	254	39	156	258	260									
Temp. °C	1200	1350	1200	1100	1050	1000	900	800									
H <sub>2</sub> O %	3.5	7.5	7.5	7.5	7.5	7.5	7.5	7.5									
Phase	Ga	Cpx	Cpx(q)	Ga	Cpx	Ga	Cpx	Zo	Ga	Cpx							
n*	4	1	3	2	6	13	range	10	range	4	5	6	3	4	1	1	3
SiO <sub>2</sub>	43.8	51.3	49.0	43.7	52.1	43.6	44.2–43.2	52.2	53.6–52.1	43.2	43.5	52.3	43.9	53.1	40.3	43.7	53.1
Al <sub>2</sub> O <sub>3</sub>	25.2	11.4	14.4	25.2	5.6	25.0	25.5–24.8	5.0	5.7–3.8	24.7	24.3	6.1	24.8	7.0	34.0	25.2	5.1
MgO	22.4	15.1	16.6	24.0	18.5	22.3	23.3–21.2	17.8	18.7–17.7	21.3	20.2	16.4	20.3	16.5	0.95	21.8	17.3
SiO <sub>2</sub>	9.7	20.9	19.7	8.1	22.9	9.9	10.3–9.3	23.5	23.9–23.2	10.4	11.7	23.7	12.2	23.1	24.9	10.8	24.0
Total	101.1	98.7	99.7	101.0	99.1	100.8		98.5		99.6	99.7	98.5	101.2	99.7	100.15	101.5	99.5

n\* = number of analytical points. Ranges of compositions measured are shown in run 254. Abbreviations, see Figure 2. q = quench crystals

Table 4. Chemical compositions, measured by microprobe analysis, of quenched glasses coexisting with garnets and clinopyroxenes in the melting interval of model quartz eclogite at 30 kbar.

Run #	144			261					254			
Temp. °C	1200			1200					1100			
H <sub>2</sub> O, Wt%	3.5			7.5					7.5			
SiO <sub>2</sub>	63.8	63.5	61.6	45.1	50.7	49.7	45.3	50.3	53.1	54.5	48.2	47.3
Al <sub>2</sub> O <sub>3</sub>	9.9	10.2	13.0	20.0	20.7	20.0	20.1	21.6	20.5	20.1	16.9	18.0
MgO	3.4	3.5	2.6	4.4	1.7	3.0	4.2	2.2	2.8	1.0	2.7	3.7
CaO	10.6	10.4	10.7	9.6	6.8	7.1	10.7	5.9	3.9	5.0	10.9	10.5
Total	87.7	87.6	87.4	79.1	79.9	79.8	80.3	80.0	80.3	80.6	78.7	79.5
Recalculated to 100%												
SiO <sub>2</sub>	72.7	72.5	69.9	57.0	63.5	62.4	56.4	62.9	66.1	67.5	61.2	59.5
Al <sub>2</sub> O <sub>3</sub>	11.3	11.6	14.8	25.4	25.9	25.0	25.1	27.0	25.6	25.0	21.5	22.6
MgO	3.9	4.0	3.0	5.5	2.1	3.8	5.3	2.7	3.4	1.3	3.4	4.6
CaO	12.1	11.9	12.3	12.1	8.5	8.8	13.3	7.4	4.9	6.2	13.9	13.3

cule are lower than at 900°C and 1000°C. This change in the trend of mineral compositions may be associated with the addition of zoisite at the temperature slightly above 900°C. The compositions of glasses measured at 1200°C and 1100°C are listed in Table 4, and plotted in Figures 3A and B. The few results with 3.5% H<sub>2</sub>O apparently show good agreement, but the wide scatter of results from runs with 7.5% H<sub>2</sub>O is beyond the analytical error. If the compositions of glasses obtained experimentally represent those of original liquids, the divergence could be attributed to local disequilibrium and inhomogeneous glasses. However, one might expect equilibrium to be achieved more readily with 7.5% H<sub>2</sub>O than with 3.5% H<sub>2</sub>O, so this explanation is not satisfactory. Evidence reviewed below suggests that the liquids experienced variable changes in composition during the quench.

The analyses of glasses total less than 100%. If the deficiencies are assumed to correspond to H<sub>2</sub>O dissolved in the H<sub>2</sub>O-undersaturated liquids at run conditions, the H<sub>2</sub>O dissolved in the 7.5% H<sub>2</sub>O runs was about 20% at 1200°C and 21% at 1100°C, and the amount in the 3.5% H<sub>2</sub>O run at 1200°C was about 12%. These values are uncertain, because of the uncertainty associated with exsolution of H<sub>2</sub>O from liquid and glass during a quench.

#### Calculated liquid compositions

Because of the problems with glass analyses at 1200°C with 7.5% H<sub>2</sub>O (Figs. 3A and B), an attempt was made to calculate the equilibrium compositions

of liquids using estimates of the modes of quenched runs and mass balance. The volumetric proportions of mineral phases and glasses in runs 261, 254, 256, and 258 with 7.5% H<sub>2</sub>O were estimated by examination of crushed fragments immersed in oils under transmitted light. Although the phase assemblages are simple, these estimates are only approximate. However, the accuracy was improved by using the measured mineral compositions for mass balance calculations to test whether the estimated amount of liquid can exist. Finally, the values listed in the first column at each temperature in Table 5 were obtained as the best estimates. Other columns at each temperature in Table 5 give a selection of modes when proportions of garnets or clinopyroxenes were changed within ±5% of the estimate. These changes shifted the proportions of liquids ±5%. The modified modes were checked by mass balance calculations. We estimate that the selected range of modes at each temperature is a reasonable approximation of the possible range of error of the calculated liquid compositions.

Comparison of the calculated liquid compositions plotted in Figures 3C and D with results in Figures 3A and B shows that the glass compositions do not correspond to the liquids present during runs at 1200°C and 1100°C. The differences are too great to be explained by analytical error. The only reasonable explanation is that the liquids were modified during the quench by clinopyroxene and garnet. Obvious quench crystals were not present in the analyzed runs. Green (1973) reported growth of rims on primary crystals during quench, but we could not detect

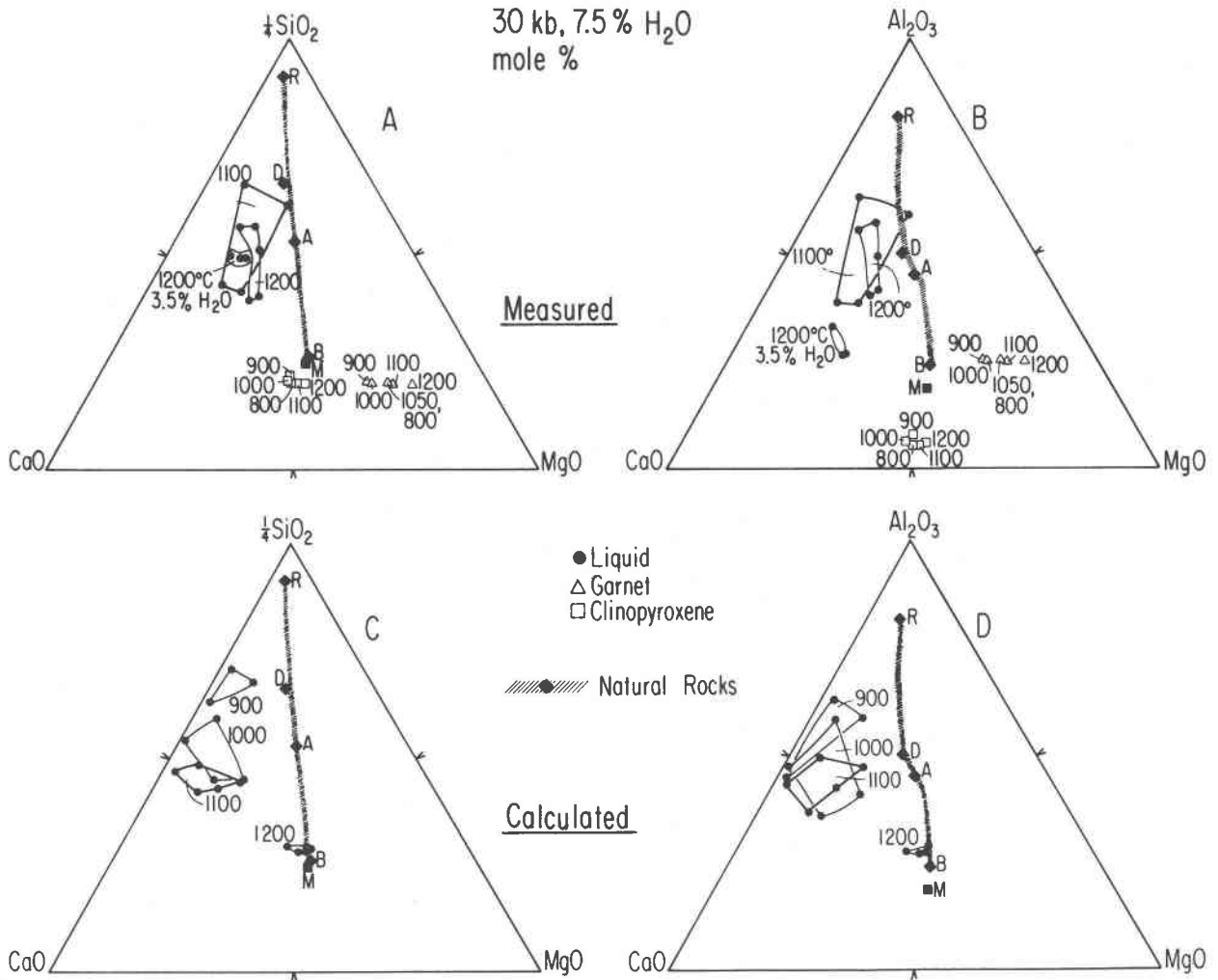


Fig. 3. For the model quartz eclogite (the solid square M) with 7.5 wt.% H<sub>2</sub>O (see Fig. 2), the measured compositions of garnets, clinopyroxenes (Table 3), and glasses (Table 4) and calculated compositions of glasses (Table 5) projected from the system CaO–MgO–Al<sub>2</sub>O<sub>3</sub>–SiO<sub>2</sub> onto two surfaces. Numbers give temperatures °C. Results for 3.5% H<sub>2</sub>O at 1200°C are also plotted in A and B. The curve BADR corresponds to the average chemical variation of calc-alkaline rocks, BADR, from Figure 1. Figures A and C are projections onto the plane CaO–MgO– $\frac{1}{4}$ SiO<sub>2</sub> (mole %). Figures B and D are projects onto the plane CaO–MgO–Al<sub>2</sub>O<sub>3</sub> (mole %).

rims on the small crystals, even with the microprobe. The problem is not resolved to our satisfaction, but we have no other explanation. The results at 1200°C with 7.5% H<sub>2</sub>O may have been especially affected by metastable precipitation of garnet, because of the proximity of the garnet phase boundary (Fig. 2). The 1200°C analyses were made on synthesis run 261, which contained garnet. Garnet was eliminated from the two-stage run at 1200°C (run 207). Therefore, the garnet produced in run 261 may be metastable, and the garnet phase boundary may be just below 1200°C.

The average value for each range of calculated liq-

uid compositions from Figures 3C and D is plotted in the same projections in Figure 4. The shaded band Mm, following these points, represents the equilibrium liquid path through the crystallization/melting interval of the model quartz eclogite M. The portion of the band from M (1360°C) to 1200°C represents the interval for Cpx + L. The path changes direction consistent with the occurrence of Cpx + Ga between 1200°C and about 950°C. The change of direction between 1000°C and 900°C (m) is associated with the appearance of zoisite, and presumably the same direction would be continued down to the solidus, at 810°C.

Table 5. Calculated liquid compositions (wt.%) through the melting interval of model quartz eclogite with 7.5% H<sub>2</sub>O

Run #	261				254					256				258		
Temp.	1200°C				1100°C					1000°C				900°C		
L	0.60	0.65	0.60	0.55	0.27	0.30	0.30	0.30	0.27	0.20	0.25	0.25	0.21	0.15	0.15	0.14
Cpx	0.35	0.35	0.40	0.35	0.48	0.50	0.45	0.40	0.43	0.50	0.45	0.40	0.44	0.50	0.45	0.51
Ga	0.05			0.10	0.25	0.20	0.25	0.30	0.30	0.30	0.30	0.35	0.35	0.30	0.30	0.30
Zo														0.05	0.05	0.05
SiO <sub>2</sub>	53.1	52.6	52.3	54.0	60.0	57.7	59.3	60.9	61.8	64.1	61.9	64.2	66.3	72.0	75.3	73.4
Al <sub>2</sub> O <sub>3</sub>	20.7	21.2	22.3	20.3	26.0	27.2	23.9	20.6	22.3	26.2	22.2	18.6	21.0	20.6	14.8	21.6
MgO	11.4	11.9	11.8	10.3	1.3	3.7	3.0	2.3	0.6	0.9	4.0	2.7	0.2	1.4	0.2	0.4
CaO	14.8	14.3	13.5	15.4	12.7	11.5	13.8	16.2	15.3	8.9	11.9	14.4	12.6	5.9	9.6	4.6

The first columns at each temperature are based on modal estimates. Other columns are calculated based on possible errors in the modes. Abbreviations, see Figure 2.

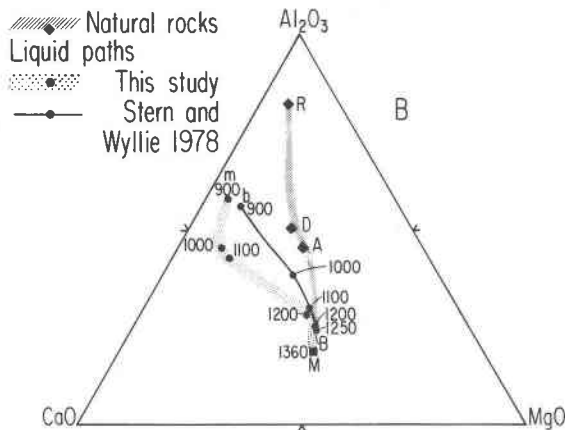
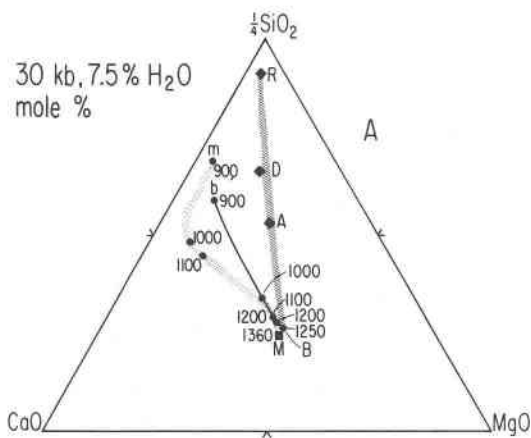


Fig. 4. Equilibrium liquid path for quartz eclogite with 7.5% wt.% H<sub>2</sub>O at 30 kbar. The line Mm is the calculated equilibrium liquid path (Figures 3C and D; Table 5) for the model quartz eclogite composition (Table 1, No. 1). The line Bb is the equilibrium liquid path for the natural rock composition (Table 1, No. 4), calculated by Stern and Wyllie (1978). A is projection onto the plane CaO-MgO- $\frac{1}{4}$ SiO<sub>2</sub> (mole %). B is projection onto the plane CaO-MgO-Al<sub>2</sub>O<sub>3</sub> (mole %).

### Comparison with results for whole rock

The results illustrated in Figures 2, 3, and 4 for the model quartz eclogite composition are similar to those published by Stern and Wyllie (1978) for a natural basalt. The compositions of the two starting materials are compared in Table 1. The experimental problems of working with Fe-bearing material were outlined above. The volatilization of alkalis from glass during electron microprobe analysis is another problem in studies on whole rock compositions. Some alkalis may be lost even before analysis, through transportation from the glass by vapor exsolving during quench.

### Phase diagram

The isobaric  $T$ - $X_{\text{H}_2\text{O}}$  diagram in Figure 2 is closely matched by the diagram presented by Stern and Wyllie (1978, Fig. 3). The vapor-absent phase relationships in the model system are much better constrained by runs than their results in the rock system. With excess H<sub>2</sub>O, the liquidus temperature for both materials is near 1100°C, but the solidus for the whole rock is at 760°C, about 40°C lower than that for the model system. In both systems, coesite disappears a few degrees above the solidus (except for low H<sub>2</sub>O contents in the vapor-absent region). Zoisite in the model system is replaced in the natural rock by kyanite. For low H<sub>2</sub>O contents, the kyanite stability extends to higher temperatures than that of zoisite. In the whole-rock system, clinopyroxene and garnet occur together at the liquidus, within the limits of experimental brackets, in contrast with the model system, where there is an extensive subliquidus region with clinopyroxene the only mineral. The liquidus boundary in the rock system is slightly higher in tem-

perature than the upper limit for Cpx + Ga in the model system. With decreasing H<sub>2</sub>O content, the liquidus in the model system is at progressively higher temperatures than that in the rock system, as the temperature interval for Cpx + L increases. Green and Ringwood (1968) gave clinopyroxene as the primary mineral for anhydrous olivine basalt at 27 kbar, with garnet appearing only 10°C below the liquidus. Because no hydrous mineral occurs in the rock system at this pressure, there is no vapor-absent solidus reaction for a partially hydrated assemblage corresponding to the melting of model zoisite-eclogite in Figure 2.

#### Mineral compositions

Compositions of garnets and clinopyroxenes through the crystallization interval of the whole rock with 7.5% H<sub>2</sub>O at 30 kbar, corresponding to the compositions plotted in Figure 3A and B for the model system, were measured or calculated by Stern and Wyllie (1978, Tables 3, 4, 6, 7, and Figs. 8, 9, 12). The closest comparison is between Figure 3A and B and their Figure 12, but direct comparison is difficult because in the rock system the garnets contain high proportions of almandine component, and the clinopyroxenes contain significant ferrosilite and jadeite components.

#### Glass-liquid composition

For the model quartz eclogite composition we concluded that the glass analyses (Figs. 3A and B) were unsatisfactory, and used calculated liquid compositions (Figs. 3C and D) to obtain the equilibrium liquid path Mm plotted in Figure 4. Stern and Wyllie (1978) measured the compositions of glasses through the crystallization interval of an andesite, but they obtained no satisfactory analytical results for the basaltic composition at 30 kbar with 5% H<sub>2</sub>O, because of extensive crystallization of quench clinopyroxene. However, they calculated the equilibrium liquid path through the crystallization interval (Stern and Wyllie, Table 8, Fig. 12). This path is projected into Figure 4A and B as the line Bb, extending from the whole-rock composition, B. Compositions were recalculated in terms of the components CaO-(MgO+FeO)-Al<sub>2</sub>O<sub>3</sub>-SiO<sub>2</sub>.

The liquid path Mm is higher in CaO/MgO for specific SiO<sub>2</sub> and Al<sub>2</sub>O<sub>3</sub> contents compared with the liquid path Bb, with the divergence greatest in the middle part of the path. There is a significant difference between the model system and the rock system with respect to the liquid compositions as a function

of temperature. The liquidus of the rock B with 7.5% H<sub>2</sub>O is about 1250° compared with about 1360°C for the model composition.

The precipitation of about 20% of Ga + Cpx from the natural composition between 1250°C and 1200°C displaces the liquid composition only a short distance from starting composition B in Figures 4A and B (compare Fig. 12 in Stern and Wyllie, 1978). For the model system, the precipitation of clinopyroxene between 1360°C and 1200°C causes a slightly greater change in liquid composition along Mm. The coprecipitation of clinopyroxene and garnet between 1200°C and 1000°C causes a greater change in liquid composition along Mm for the model system than along Bb for the natural rock system.

#### Discussion

The availability of H<sub>2</sub>O in subducted oceanic crust exerts significant control over magmatic processes. In most thermal models for subduction zones, it is difficult to devise schemes to transport H<sub>2</sub>O much deeper than 150 km (e.g., Wyllie, 1973, 1979). The occurrence of zoisite within the fusion interval for the synthetic composition (Fig. 1) suggests the possibility that zoisite, or epidote, is capable of transporting H<sub>2</sub>O within subducted oceanic crust to deeper levels than amphibole stability. In their study of gabbro-H<sub>2</sub>O, Lambert and Wyllie (1972) suspected the presence of zoisite in their runs, but could not prove it. Stern and Wyllie (1978) found no zoisite or epidote in the same gabbro at 30 kbar. Green (1980) presented experimental evidence that zoisite in gabbroic compositions is restricted to pressures and temperatures within the amphibole stability field.

The calculated equilibrium liquid paths for the model and natural rock compositions are compared in Figure 4 with the average chemical variation of the calc-alkaline rock series, BADR. Both paths diverge from the composition line for the natural rock series, and the divergence for the model system (Mm) is greater than that for the natural rock system (Bb).

According to these liquid paths, the partial fusion of quartz eclogite in the presence of a few per cent H<sub>2</sub>O at 100 km depth would produce first a water-saturated liquid with higher SiO<sub>2</sub> content than that of andesite (Green and Ringwood, 1972; Stern and Wyllie, 1973, 1978). With progressive fusion, free vapor would be dissolved within a few degrees of the solidus (Fig. 1), and H<sub>2</sub>O-undersaturated liquid could coexist with residual eclogite through hundreds of degrees above the solidus (Fig. 1; Stern and Wyllie, Fig. 3). With increase in temperature, the liquid

composition changes by increase in CaO, MgO, and FeO, and by decrease in alkalis,  $\text{Al}_2\text{O}_3$ , and  $\text{SiO}_2$  (Fig. 4; Stern and Wyllie, 1978, Table 8). For both model and natural rock compositions, a liquid with intermediate  $\text{SiO}_2$  content corresponding to that of an andesite is produced at a temperature near  $950^\circ\text{C}$ ,  $150\text{--}200^\circ\text{C}$  above the solidus, where the estimated percentage of liquid is about 20–25%. The liquid composition at this stage has considerably higher CaO/MgO or CaO/(MgO + FeO) than the andesite represented on the average chemical variation line BADR for calc-alkaline rocks. There is no special region within the phase diagrams (Fig. 1; Stern and Wyllie, 1978, Fig. 3) to suggest that large quantities of liquid with intermediate  $\text{SiO}_2$  content are produced within a narrow temperature interval. These liquids are produced as part of a continuous variation from the siliceous liquids to basaltic liquids. It is only in the upper part of the wide fusion interval for quartz eclogite that the liquids with  $\text{SiO}_2$  and  $\text{Al}_2\text{O}_3$  contents corresponding to basaltic andesites and basalts become similar to the rock series in Ca/(Mg + Fe).

These results reinforce the conclusion of Stern and Wyllie (1978) that the partial melting of quartz eclogite in subducted oceanic crust at 100 km depth would produce liquids with a range of high to intermediate  $\text{SiO}_2$  contents, but with Ca/(Mg + Fe) higher than that in the calc-alkaline rock series. We conclude, therefore, that andesite is not a primary magma from subducted oceanic crust at depths greater than amphibole breakdown. Given the very wide fusion interval in the presence of  $\text{H}_2\text{O}$  (Fig. 2), it seems more likely that hydrous, siliceous magmas would leak from the subducted oceanic crust into overlying mantle, as proposed by Nicholls and Ringwood (1973).

Marsh (1979) presented a scheme where convection in the mantle wedge overlying the subducted lithosphere is so vigorous that the  $1,250^\circ\text{C}$  isotherm extends into the oceanic crust at 100 km depth. These are the conditions required if basaltic-andesite magma with low  $\text{H}_2\text{O}$  content is to be produced at this depth. Some aspects of this model can be evaluated on the basis of the phase diagrams. High temperature gradients would exist at somewhat shallower depths, and the wide temperature interval for progressive fusion indicated in Figure 2 (Stern and Wyllie, 1978, Fig. 3) could therefore be compressed into a narrow depth interval. This might delay the escape of liquid into the overlying mantle until the high degree of partial fusion required to generate ba-

saltic andesites had been achieved. However, the subducted oceanic crust is much hotter than in other geophysical models, and the petrological implications for greater depths need evaluation.

In order to elucidate the details of hybridization reactions between rising melts and the overlying peridotite, we need to know the compositions of liquids generated during the early stages of partial fusion, but the precise compositions of liquids generated within the first  $100\text{--}200^\circ\text{C}$  of partial fusion remain undetermined. We could make no satisfactory measurements of glass compositions below  $1100^\circ\text{C}$ , and calculations below  $900^\circ\text{C}$  were considered to be unreliable.

If the compositions of near-solidus liquids within a single bulk composition cannot be measured or calculated, an alternative approach is to determine the liquidus field boundaries and invariant points within the system CaO–MgO– $\text{Al}_2\text{O}_3$ – $\text{SiO}_2$ – $\text{H}_2\text{O}$ . Most previous experimental attention to this system at high pressures has been devoted to phase relationships related to basalts and peridotites, with studies near the  $\text{MgSiO}_3$ – $\text{CaSiO}_3$ – $\text{Al}_2\text{O}_3$  join ( $\pm\text{Mg}_2\text{SiO}_4$ ), and the bounding system  $\text{Mg}_2\text{SiO}_4$ – $\text{CaMgSi}_2\text{O}_6$ – $\text{SiO}_2$ . We have underway experiments for determination of the flow chart near the  $\text{SiO}_2$  corner of the system, with a view to tracing paths of fusion (or crystallization) involving the minerals quartz/coesite, garnet, and pyroxene (Sekine and Wyllie, 1980).

### Acknowledgment

This research was supported by the Earth Sciences Section, National Science Foundation, grant EAR 76-20413. Reviews by A. L. Boettcher and A. Navrotsky were very helpful.

### References

- Allen, J. C. and Boettcher, A. L. (1978) Amphiboles in andesite and basalt: II. Stability as a function of  $P$ – $T$ – $f_{\text{H}_2\text{O}}$ – $f_{\text{O}_2}$ . *American Mineralogist*, 63, 1074–1087.
- Allen, J. C., Boettcher, A. L., and Marland, G. (1975) Amphiboles in andesite and basalt: I. Stability as a function of  $P$ – $T$ – $f_{\text{O}_2}$ . *American Mineralogist*, 60, 1069–1085.
- Anderson, R. N., DeLong, S. E., and Schwartz, W. M. (1978) Thermal model for subduction with dehydration in the downgoing slab. *Journal of Geology*, 86, 731–739.
- Anderson, R. N., DeLong, S. E., and Schwartz, W. M. (1980) Dehydration, asthenospheric convection and seismicity in subduction zones. *Journal of Geology*, 88, 445–451.
- Boettcher, A. L. and Wyllie, P. J. (1969) Phase relationships in the system  $\text{NaAlSi}_3\text{O}_8$ – $\text{SiO}_2$ – $\text{H}_2\text{O}$  to 35 kilobars pressure. *American Journal of Science*, 267, 875–909.
- Carmichael, I. S. E., Turner, F. J., and Verhoogen, J. (1974) *Igneous Petrology*. McGraw-Hill, New York.
- Engel, A. E. J., Engel, C. G., and Havens, R. G. (1975) Chemical characteristics of oceanic basalts and the upper mantle. *Geological Society of America Bulletin*, 76, 719–734.

- Green, D. H. (1973) Experimental melting studies on model upper mantle compositions at high pressure under both water-saturated and water-undersaturated conditions. *Earth and Planetary Science Letters*, 19, 37–53.
- Green, D. H. (1976) Experimental testing of "equilibrium" partial melting of peridotite under water-saturated, high-pressure conditions. *Canadian Mineralogist*, 14, 255–268.
- Green, T. H. (1972) Crystallization of calc-alkaline andesite under controlled high-pressure hydrous conditions. *Contributions to Mineralogy and Petrology*, 34, 150–166.
- Green, T. H. (1980) Island arc and continent building magmatism—a review of petrogenic models based on experimental petrology and geochemistry. *Tectonophysics*, 63, 367–385.
- Green, T. H. (1981a) Experimental studies relevant to petrogenesis of andesites: (a) Anatexis of mafic crust and high pressure crystallization of andesite. In R. S. Thorpe, Ed., *Andesites and Related Rocks*, Wiley, in press.
- Green, T. H. (1981b) Experimental evidence for the role of accessory phases in magma genesis. *Journal of Volcanology and Geothermal Research*, in press.
- Green, T. H. and Ringwood, A. E. (1968) Genesis of the calc-alkaline igneous rocks suite. *Contributions to Mineralogy and Petrology*, 18, 105–162.
- Green, T. H. and Ringwood, A. E. (1972) Crystallization of garnet bearing rhyodacite under high-pressure hydrous conditions. *Journal of Geological Society of Australia*, 19, 203–212.
- Herzberg, C. T. (1976) X-ray method for determination of clinopyroxene compositions in the system  $\text{CaO-MgO-Al}_2\text{O}_3\text{-SiO}_2$ . In G. M. Biggar, Ed., *Progress in Experimental Petrology*, 3rd, p. 239–241. Nat. Envir. Res. Council.
- Huang, W.-L. and Wyllie, P. J. (1975) Melting reactions in the system  $\text{NaAlSi}_3\text{O}_8\text{-KAlSi}_3\text{O}_8\text{-SiO}_2$  to 35 kilobars, dry and with excess water. *Journal of Geology*, 83, 737–748.
- Kay, R. W. (1980) Volcanic arc magmas: Implications of a melting-mixing model for element recycling in the crust-upper mantle system. *Journal of Geology*, 88, 497–522.
- Kay, R. W., Hubbard, N. J., and Gast, P. W. (1970) Chemical characteristics and origin of oceanic ridge volcanic rocks. *Journal of Geophysical Research*, 75, 1585–1613.
- Lambert, I. B. and Wyllie, P. J. (1972) Melting of gabbro (quartz eclogite) with excess water to 35 kilobars, with geological applications. *Journal of Geology*, 80, 693–708.
- Lambert, I. B. and Wyllie, P. J. (1974) Melting of tonalite and crystallization of andesite liquid with excess water to 30 kilobars. *Journal of Geology*, 82, 88–97.
- Luth, W. C. and Ingamells, C. O. (1965) Gel preparation of starting materials for hydrothermal experiments. *American Mineralogist*, 50, 255–258.
- Macdonald, G. A. and Katsura, T. (1964) Chemical compositions of Hawaiian lavas. *Journal of Petrology*, 5, 82–133.
- Marsh, B. (1979) Island-arc volcanism. *American Scientist*, 67, 161–172.
- Merrill, R. B. and Wyllie, P. J. (1973) Iron absorption by platinum capsules in high pressure rock melting experiments. *American Mineralogist*, 58, 16–20.
- Nehru, C. E. and Wyllie, P. J. (1975) Compositions of glasses from St. Paul's peridotite partially melted at 20 kilobars. *Journal of Geology*, 83, 455–471.
- Newton, R. C., Charlu, T. V., and Kleppa, O. J. (1977) Thermochemistry of high-pressure garnets and clinopyroxenes in the system  $\text{CaO-MgO-Al}_2\text{O}_3\text{-SiO}_2$ . *Geochimica et Cosmochimica Acta*, 41, 369–377.
- Nicholls, I. A. and Ringwood, A. E. (1973) Effect of water on olivine stability in tholeiites and the production of silica-saturated magmas in the island arc environment. *Journal of Geology*, 81, 285–300.
- Raheim, A. and Green, D. H. (1974) Experimental determination of the temperature and pressure dependence of the Fe-Mg partition coefficient for coexisting garnet and clinopyroxene. *Contributions to Mineralogy and Petrology*, 48, 179–203.
- Reed, S. J. B. and Ware, N. G. (1975) Quantitative electron microprobe analysis of silicates using energy-dispersive X-ray spectrometry. *Journal of Petrology*, 16, 499–519.
- Sekine, T. and Wyllie, P. J. (1980) Melting relations in the system  $\text{Pyr}_1\text{Gross}_2\text{-Pyr}_2\text{Gross}_1\text{-Qtz-H}_2\text{O}$  at 30 kb. (abstr.) *EOS*, 61, 396.
- Stern, C. R. (1974) Melting products of olivine tholeiite basalt in subduction zones. *Geology*, 2, 227–230.
- Stern, C. R. and Wyllie, P. J. (1973) Melting relations and basalt-andesite-rhyolite- $\text{H}_2\text{O}$  and a pelagic red clay at 30 kilobars. *Contributions to Mineralogy and Petrology*, 42, 313–323.
- Stern, C. R. and Wyllie, P. J. (1975) Effect of iron absorption by noble-metal capsules on phase boundaries in rock melting experiments at 30 kb. *American Mineralogist*, 60, 681–689.
- Stern, C. R. and Wyllie, P. J. (1978) Phase compositions through crystallization intervals in basalt-andesite- $\text{H}_2\text{O}$  at 30 kbar with implication for subduction zone magmas. *American Mineralogist*, 63, 641–663.
- Stern, C. R., Huang, W.-L., and Wyllie, P. J. (1975) Basalt-andesite-rhyolite- $\text{H}_2\text{O}$ : crystallization intervals with excess  $\text{H}_2\text{O}$  and  $\text{H}_2\text{O}$ -undersaturated liquidus surfaces to 35 kilobars, with implications for magma genesis. *Earth and Planetary Science Letters*, 28, 189–196.
- Wyllie, P. J. (1973) Experimental petrology and global tectonics: a preview. In P. J. Wyllie, Ed., *Experimental petrology and global tectonics*. *Tectonophysics*, 17, 189–209.
- Wyllie, P. J. (1978) Water and magma generation at subduction zones. *Bulletin Volcanologique*, 41, 360–377.
- Wyllie, P. J. (1979) Magmas and volatile components. *American Mineralogist*, 64, 469–500.
- Wyllie, P. J. (1981) Subduction products according to experimental prediction. *Bulletin Geological Society of American*, in press.
- Yagi, K., Kawano, Y., and Aoki, K. (1963) Types of Quaternary volcanic activity in northeastern Japan. *Bulletin Volcanologique*, 26, 223–235.

*Manuscript received, February 6, 1981;  
accepted for publication, May 25, 1981.*